Physics in Medicine & Biology

Preliminary dosimetric analysis of DOTA-folate radiopharmaceutical radiolabelled with ^{47}Sc produced through ^{nat}V(p,x)^{47}Sc cyclotron irradiation

To cite this article before publication: Laura De Nardo *et al* 2020 *Phys. Med. Biol.* in press https://doi.org/10.1088/1361-6560/abc811

Preliminary dosimetric analysis of DOTA-folate radiopharmaceutical radiolabelled with ^{47}Sc produced through ^{nat}V(p,x)^{47}Sc cyclotron irradiation.

L. De Nardo[1,2*], G. Pupillo[3], L. Mou[3], D. Furlanetto[1], A. Rosato[4,5], J. Esposito[3] and L. Meléndez-Alafort[5]

[1]*Department of Physics and Astronomy, University of Padova, Via Marzolo 8, Padova, 35131, Italy*

[2]*INFN (Istituto Nazionale di Fisica Nucleare), Sezione di Padova, Via Marzolo 8, Padova, 35131, Italy*

[3]*INFN, Legnaro National Laboratories (LNL), Viale dell'Università 2, Legnaro, 35020, Italy*

[4]*Department of Surgery, Oncology and Gastroenterology, University of Padova, Via Gattamelata 64, Padova, 35138, Italy*

[5]*Veneto Institute of Oncology IOV-IRCCS, Via Gattamelata 64, Padova, 35138, Italy*

**Corresponding author: laura.denardo@unipd.it*

Keywords: ^{47}Sc-labeled radiopharmaceutical · Theranostic radionuclides · Cyclotron-induced reactions · Internal dosimetry

Abstract

^{47}Sc is one of the most promising theranostic radionuclides, thanks to its low energy γ-ray emission (159 keV), suitable for SPECT imaging and its intense β^- emission, useful for tumor treatment. Despite promising preclinical results, the translation of ^{47}Sc-therapeutic agents to the clinic is hampered by its limited availability. Among different ^{47}Sc-production routes currently being investigated, the ^{nat}V(p,x)^{47}Sc reaction has proved to be of particular interest, thanks to the low-cost and easy availability on the market of ^{nat}V material and the diffusion of medium energy proton cyclotrons. However, the cross section of this specific nuclear reaction is quite low and small amounts of Sc-contaminants are co-produced at energies $E_P \leq 45$ MeV, namely ^{48}Sc and ^{46}Sc. The main concern with these Sc-contaminants is their contribution to the patient absorbed dose. For such a reason, the absorbed dose contributions to healthy organs and the effective dose contributions by the three radioisotopes, ^{48}Sc, ^{47}Sc and ^{46}Sc, were evaluated using DOTA-folate conjugate (cm10) as an example of radiopharmaceutical product. Considering as acceptable the limits of 99%

for the radionuclidic purity and 10% for the contribution of radioactive Sc-contaminants to the total effective dose after ^{47}Sc-cm10 injection, it was obtained that proton beam energies below 35 MeV must be used to produce ^{47}Sc through irradiation of a ^{nat}V target.

1. Introduction

The term theranostics in nuclear medicine specifies the administration of a radiopharmaceutical product to obtain both a molecular image of a cancer disease and a therapeutic effect. By using a theranostic agent it is feasible to study the radiopharmaceutical biodistribution, to accurately determine each organ kinetics and to precisely calculate the absorbed dose received by the target organs and the total body. Consequently, this approach results in a more personalized therapy (Yordanova *et al* 2017). The major advantage of theranostics relies on the possibility to select the patients that positively respond to the specific treatment, by performing low-activity imaging prior the therapy. In general, theranostic radiopharmaceuticals are formed by a targeting vector labelled with radionuclides that allow to specifically visualize and irradiate tumors thanks to their physical decay characteristics. Commonly, radionuclides that emit radiation mainly resulting in energy deposition close to the decay point, such as α or low energy β^- particles, are used for therapy, while β^+ or γ-radiation emitters are used for imaging, respectively for positron emission tomography (PET) or single photon emission computed tomography (SPECT).

Recently, production routes of new radionuclides with ideal characteristics for imaging and also suitable for therapy have been studied. ^{47}Sc ($\tau_{1/2}$ = 3.35 d (NNDC 2020)) is a fast-developing example of an excellent theranostic radionuclide thanks to the 159 keV γ-ray suitable for SPECT imaging and the intense β^- emission ($\bar{E}_{\beta^-}$ = 162.0 keV), useful to treat small-size tumours. Sc has also got two β^+ emitting isotopes, ^{43}Sc and ^{44g}Sc ($\tau_{1/2}$ = 3.891 h and 3.97 h respectively (NNDC 2020)), that are good alternatives for PET imaging (Notni and Wester 2018). In addition to this, the stable coordination of Sc element with the chelating agent DOTA makes ^{47}Sc suitable for labelling DOTA-derivatized biomolecules, currently available for diagnosis, for future applications as theranostic agents (Mikolajczak *et al* 2019).

The therapeutic potential of ^{47}Sc has been proven at preclinical level (Müller *et al* 2014, Siwowska *et al* 2019), but unfortunately the limited availability has slowed down the research and the translation of ^{47}Sc-therapeutic agents to the clinic. Currently, ^{47}Sc is being produced in nuclear reactors by neutron-induced reactions, mainly from enriched Ca or Ti targets, with high Radionuclidic Purity (RNP) (>99%). However, due to the limited number of nuclear reactors and the expensive cost of the target material needed, new cyclotron-based production routes of ^{47}Sc are currently being studied (Qaim *et al* 2018, IAEA 2014). In particular, experimental studies considering the ^{nat}V(p,x)^{47}Sc reaction at medium energy proton beams were conducted within the framework of the "Production with Accelerator of ^{47}Sc for Theranostic Applications (PASTA)" research project, funded by INFN at the National Laboratories of Legnaro (INFN-LNL) (Pupillo *et al* 2019). Results have demonstrated that this alternative production route is of particular interest, due to the low-cost of the commercially easily available ^{nat}V targets (^{50}V, 0.250% and ^{51}V, 99.750%) and the diffusion of medium energy proton cyclotrons. However, the nuclear cross section of the ^{nat}V(p,x)^{47}Sc reaction is quite low (approximately 12 mb at about 35 MeV) and small amounts of other Sc-isotopes are co-produced. The activity at the End Of Bombardment (EOB) of ^{47}Sc and contaminant Sc-radioisotopes basically depends on the proton beam energy, the target isotopic composition and the irradiation time.

In general, the presence of contaminant-isotopes in the solution used to label a radiopharmaceutical does not change the labelling efficiency, the radiochemical purity or the biological behaviour after administration. The main problem with the radioisotopic contaminants is their contribution to the exposure of the patient to ionizing radiation, resulting in increased effective dose and, for therapeutic applications, increased absorbed doses to risk organs. This contribution directly depends on the biodistribution and the kinetics of each radiopharmaceutical used (Meléndez-Alafort *et al* 2019). Therefore, new radiopharmaceuticals must be fully characterized before their clinical use, especially when they are labelled with novel radionuclides. The European Pharmacopoeia requires that the radiopharmaceutical purity is enough to guarantee a safe clinical application. This is not an issue when the impurities are radionuclides of other elements, because they can be removed

chemically. However, when the impurities are radioisotopes, they remain in the final product, because the chemical purification process is not possible. Therefore, radionuclides production methods must generate a minimal amount of radioisotopes to keep the presence of impurities at as low as acceptable levels (EANM 19). In general, the radionuclidic impurities limit is usually expressed as a percentage and from a pharmaceutical/Good Manufacturing Practice (GMP) viewpoint it should be set lower than 1%. However, this limit can be drastically reduced, if very high-purity products are technically achievable with the production process, as in the case of ^{18}F, for which the radionuclidic impurities limit is 0.1% (EDQM 2018). To establish the minimal purity of new radiopharmaceuticals labelled with cyclotron-produced (CP) radionuclides, it must be considered not just the percent of radionuclidic impurities produced (<1%), but also the Dose Increase (DI) caused by these impurities. Nowadays, there is not an established limit for the DI, but in general 10% is considered a good starting value to set the limits of the impurities. As an example, the draft of the sodium pertechnetate ^{99m}Tc-CP monograph stated that the DI would be maintained within this 10% limit and this led to establish the maximum limit of impurities much lower than the 1% value allowed by GMP. However, the final version of the monograph published in the pharmacopeia (European Pharmacopoeia 2018) does not mention explicitly this 10% limit because, if all the impurities are kept under their established limits, it is guaranteed that the DI will be lower than 10%. In addition, since the radionuclidic purity changes with time due to the differences in the half-lives of the different radioisotopes present in a preparation, the requirements of the radionuclidic purity must be fulfilled not only at the time of testing, but throughout the period of validity of the radiopharmaceutical (EDQM 2018). In the absence of established radionuclidic impurities limits concerning the production of ^{47}Sc, in this work the two mentioned criteria, RNP>99% and DI<10%, will be examined. The comparison between these two criteria will also show which one is more restrictive for the considered ^{47}Sc-labelled radiopharmaceutical.

The DOTA-folate conjugate cm10 labelled with ^{47}Sc (^{47}Sc-cm10) is one of the ^{47}Sc-complexes better described in the literature (Siwowska *et al* 2019, Müller *et al* 2014). The cm10 is composed by a targeting vector folic acid (which selectively binds to the folate receptor

expressed on a variety of tumor types), the chelating agent DOTA and a small-molecular-weight albumin, which improves the blood circulation time and tissue distribution profile of folate conjugates. Detailed ^{47}Sc-cm10 biodistribution data based on SPECT/CT images have been reported, demonstrating high localization in the tumor site (Müller *et al* 2014). This information has been used in the current study to determine the ^{47}Sc-cm10 kinetics data necessary to calculate the effective dose produced by this radiopharmaceutical.

The aim of this work is therefore to determine the irradiation conditions capable to produce ^{47}Sc by ^{nat}V(p,x)^{47}Sc reaction with the best compromise between activity and purity. Moreover, to establish the time window after the EOB in which ^{47}Sc could be used to label a radiopharmaceutical with an acceptable radionuclidic purity (>99%) and DI (<10%) to the patient, the more restrictive criterion will be considered. ^{47}Sc-cm10 complex was used as an example of radiopharmaceutical to perform this task.

2. Methods

2.1 Calculation of radioisotopes yields due to ^{nat}V(p,x)^{XX}Sc nuclear reactions

The production yields of ^{XX}Sc radionuclides were calculated considering different irradiation conditions, such as energy window and irradiation time, using the formula reported in the IAEA Technical report series No. 468 (IAEA 2009):

$$Y_{EOB}=\frac{N_A I}{A_T}\left(1-e^{-\lambda t}\right)\int_{E_E}^{E_I}\sigma_T(E)\frac{dE}{S_T(E)} \quad (1)$$

where Y_{EOB} is the thick target Yield (Y) or the number of produced nuclei at the EOB, N_A is the Avogadro constant, I is the incident particle flux per second and it is related to the beam current, A_T is the atomic weight of the target material in grams, λ is the decay constant of the radionuclide of interest, t is the irradiation time, E_I and E_E are the Incident and Exit energy of the beam on/out of the target respectively, $\sigma_T(E)$ is the cross section for the radionuclide production at the energy E, $S_T(E)$ is the stopping power of the particle beam through the target material at the energy E, usually expressed as dE/dx. The term $(1-e^{-\lambda t})$, called Saturation Factor (SF), represents the competition of the production of the radionuclide of interest and its radioactive decay, occurring during the irradiation time. The

SF directly depends on the radionuclide half-life ($\tau_{1/2} = ln2/\lambda$) and it allows the determination of the time necessary to obtain a given production of the desired radionuclide, assuming 100% as the saturated yield, i.e. the maximum yield achievable, corresponding to the equilibrium between the number of produced and decaying nuclei. For example, an irradiation time of one half-life ($t = \tau_{1/2}$) or two half-lives ($t = 2\tau_{1/2}$) respectively provides 50% and 75% of the saturated yield. For practical reasons, irradiation times rarely exceed three half-lives, corresponding to 90% of the saturated yield, except for the shortest-lived radioisotopes (IAEA 2008).

The first step in the calculation was to determine the cross section values for each radionuclide as a function of the proton energy, ranging from 19 MeV up to 45 MeV. The lower energy limit was chosen as it corresponds to the rise of the cross section value for the $^{nat}V(p,x)^{47}Sc$ nuclear reaction route (Pupillo *et al* 2019), while the higher energy value was chosen in order to limit as much as possible the co-production of additional contaminant radioisotopes, such as ^{43}Sc, ^{44m}Sc, ^{44g}Sc, ^{46}Sc and ^{48}Sc. Yield values were obtained for each radionuclide considering a polynomial fit of the experimental data extracted from the EXFOR database (EXFOR 2020); the recent cross section values measured in the framework of the PASTA project (Pupillo *et al* 2019), including some unpublished values for the $^{nat}V(p,x)^{48}Sc$ cross section, were also considered in the fit.

Calculations were carried out considering irradiation times of 24 hours and 80 hours, corresponding to 19% ($t = 0.3\times\tau_{1/2}$) and 50% ($t = 1.0\times\tau_{1/2}$) respectively of the saturated yield for ^{47}Sc production and for different energy windows, that is E_I - E_E intervals. In particular, the exit energy E_E was fixed to 19 MeV in the (1) formula, while the upper limit, i.e. the incident beam energy E_I, was varied (30, 35, 40, 45 MeV). In this work only calculations were performed but in the future some experiments are scheduled with a Thick Target. In that case, the E_I proton energy will be directly chosen with the cyclotron while the E_E exit energy will be determined by the proper thickness of the target.

2.2 Determination of the number of disintegrations in the source organs due to ^{XX}Sc-cm10 injection

Biodistribution data in KB tumor-bearing nude mice after ^{47}Sc-cm10 injection (Müller *et al* 2014) were used to calculate the activity curves in the main male human organs through the relative mass scaling method, which takes into account the differences in human and animal organ masses compared to the total body masses (Sparks and Aydogan 1999). First, the radiopharmaceutical concentrations in the source organs, reported as percent of injected activity per gram of tissue ($[\%IA/g]_A$), were scaled from mice to humans through the following formula:

$$\left(\frac{\%IA}{organ}\right)_H = \left(\frac{\%IA}{g}\right)_A \cdot \frac{OW_H}{TBW_H} \cdot TBW_A \quad (2)$$

where OW_H is the human organ weight, TBW_A and TBW_H are the average total body weight for animal and human, respectively. OW_H and TBW_H values were obtained from the male phantom reported in ICRP 89 (ICRP 2002). The activity reported by Muller et al. as *[%IA/g]* in "blood" was assigned to "heart contents" using eq. (2).

The decay-corrected percent of injected activity for each human source organ were then plotted as a function of post injection (p.i.) time and fitted by a tri-exponential equation, which represents the phase of accumulation and the possibility of both a fast and a slow elimination of the radiopharmaceutical, with CoKiMo software (Meléndez-Alafort *et al* 2017). At last, the number of disintegrations per unit administered activity in the source organs was calculated through the software by integration of organ activity curves, considering the physical half-lives of each radioisotope.

2.3 Assessment of organ absorbed doses and effective dose due to ^{XX}Sc-cm10 injection

Dosimetric calculations were performed with OLINDA (Organ Level Internal Dose Assessment) software code version 2.1.1 (Stabin and Farmer, 2012; Stabin et al., 2005). This code utilizes realistic NURBS-type models (Stabin *et al* 2012), based on the standardized masses defined by ICRP 89 (ICRP 2002) to obtain the absorbed doses per unit of administered activity in each organ using the RADAR method for internal dose estimation (Stabin and Siegel 2017). The input were the number of disintegrations in the source organs per unit of administered activity (MBq×h/MBq) and the tabulated dose factors that depend on the radioisotope, the spatial relationship between the target and the source organ and

their tissue composition.

For each ^{xx}Sc-radioisotope *i*, the effective dose, ED_i per unit of administered activity was obtained as the sum of the product of equivalent dose and the tissue-weighting factor recommended by ICRP 103 (ICRP 2007) for each organ.

Finally, the total effective dose (ED_t) of Sc-cm10 was calculated considering that the radiopharmaceutical was injected immediately after labelling with the mixtures of Sc-radioisotopes present at the different times after EOB, using the following equation:

$$ED_t(t) = \sum_i f_i(t) ED_i \quad (3)$$

where $f_i(t)$ is the fraction of total activity corresponding to each radioisotope *i* at the time t after EOB.

3. Results

3.1 Calculated yields of ^{47}Sc and contaminant radionuclides (^{46}Sc and ^{48}Sc)

Polynomial fits of the available experimental data up to 50 MeV were used to obtain an expression of the dependence of the cross sections against the proton energy, E_P. Figure 1 shows the cross sections data for the ^{nat}V(p,x)^{XX}Sc reactions vs. proton energy used to obtain the fits. Plots demonstrate that the co-production of ^{48}Sc is negligible for E_P < 35 MeV (see fig 1(a)).

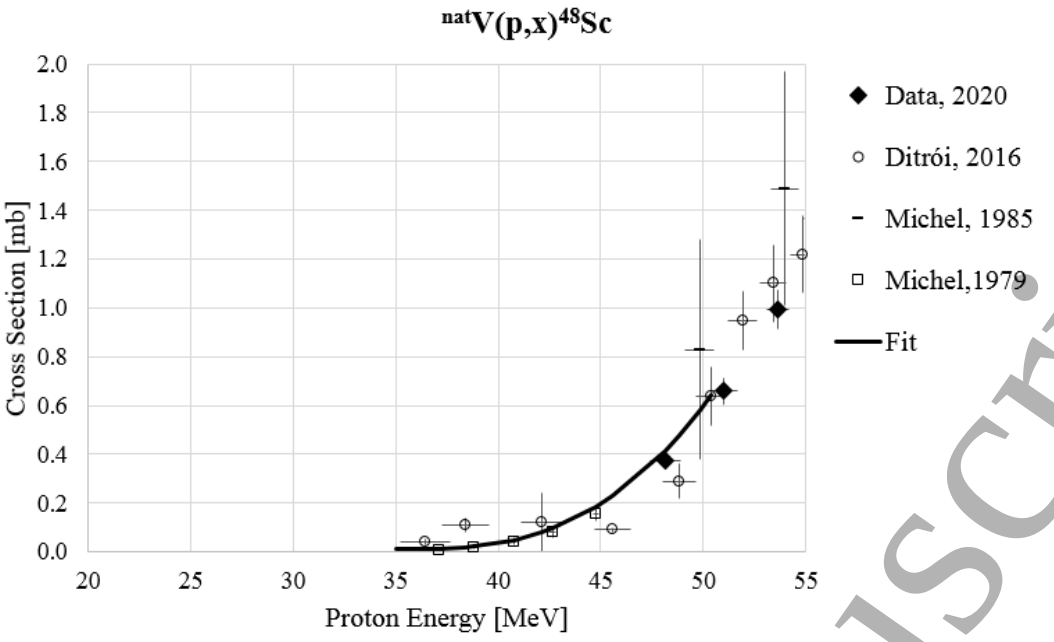

(a)

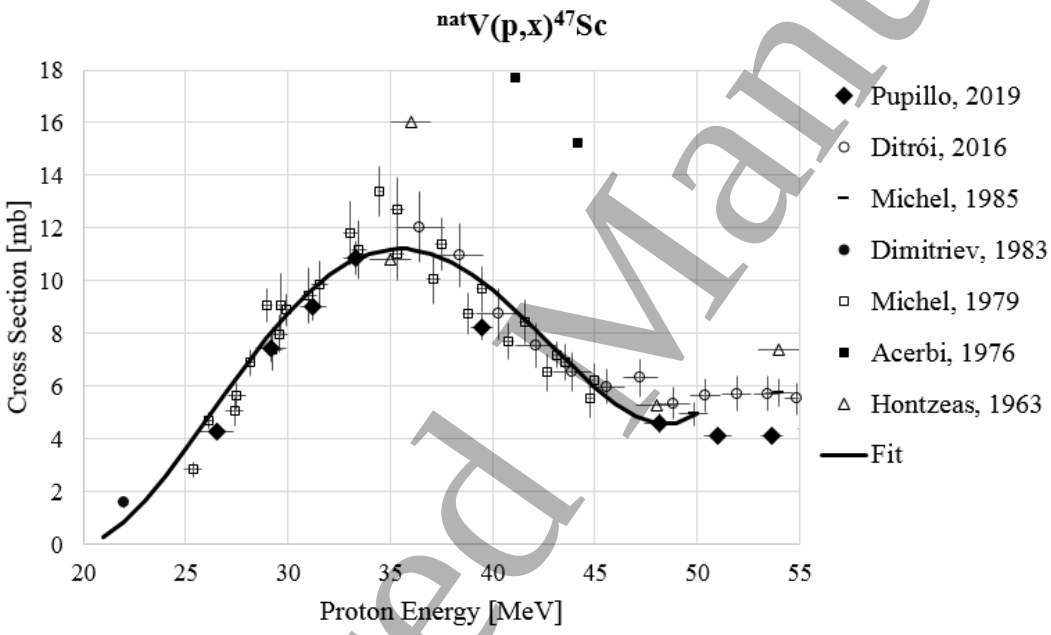

(b)

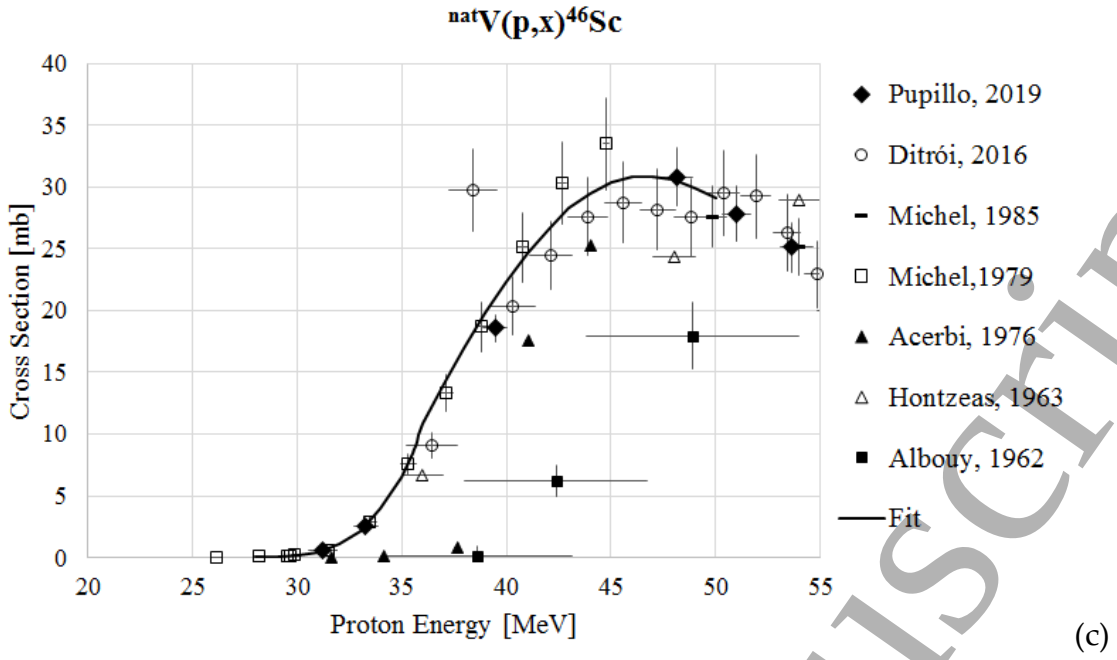

(c)

Figure 1. *Polynomial fits up to 50 MeV of the $^{nat}V(p,x)^{48}Sc$, ^{47}Sc, ^{46}Sc nuclear cross sections of literature experimental data and values measured in the framework of the PASTA project (Data 2020: G. Pupillo, unpublished data).*

The calculated production yields at EOB of ^{47}Sc and contaminants (^{48}Sc and ^{46}Sc) are presented in table 1 and refer to different energy ranges, considering 1 μA as proton beam current and irradiation times of 24 hours and 80 hours. Table 1 also presents the RNP of ^{47}Sc at the EOB for every irradiation condition considered.

Table 1. *Production yields at EOB of ^{47}Sc and contaminants (^{46}Sc, ^{48}Sc), calculated for 1 μA proton beam impinging on ^{nat}V thick target for different irradiation parameters.*

Irradiation time: t = 24 hours				
Energy range (MeV)	^{48}Sc (Bq)	^{47}Sc (Bq)	^{46}Sc (Bq)	^{47}Sc RNP (%)
45-19	1.74×10^{6}	2.37×10^{8}	1.49×10^{7}	93.43
40-19	1.95×10^{5}	1.75×10^{8}	5.14×10^{6}	97.04
35-19	-	1.05×10^{8}	6.45×10^{5}	99.39
30-19	-	4.15×10^{7}	1.49×10^{4}	99.96
Irradiation time: t = 80 hours				

Energy range (MeV)	^{48}Sc (Bq)	^{47}Sc (Bq)	^{46}Sc (Bq)	^{47}Sc RNP (%)
45-19	3.94×10^{6}	6.31×10^{8}	4.93×10^{7}	92.22
40-19	4.43×10^{5}	4.67×10^{8}	1.70×10^{7}	96.40
35-19	-	2.79×10^{8}	2.13×10^{6}	99.24
30-19	-	1.11×10^{8}	4.92×10^{4}	99.96

As expected, the highest ^{47}Sc activity is produced using the larger energy window (i.e. 45-19 MeV) and the longer irradiation time (i.e. 80 h), but in these conditions the initial RNP of ^{47}Sc is only 92.22%. The initial RNP increases by reducing the energy of the beam impinging over the target: when the proton energy range is restricted to 35-19 MeV, the amount of ^{47}Sc activity produced is reduced, but the initial RNP is higher than 99%. This value becomes higher than 99.9% in the energy range 30-19 MeV, but the amount of ^{47}Sc activity produced is quite low, about 41.5 MBq (1.1 mCi) for 24 h irradiation and about 111 MBq (3 mCi) for 80 h irradiation. Among both Sc-contaminants produced, ^{46}Sc is the radionuclide of major concern, due to its long half-life (see table 2). The main decay characteristics of ^{48}Sc, ^{47}Sc, ^{46}Sc from the dosimetric point of view (product of radiation energy times the probability per disintegration larger than 0.01 MeV/(Bq×s)) are reported in Table 2 (NNDC 2020).

Table 2. *Main decay characteristics of ^{48}Sc, ^{47}Sc, ^{46}Sc.*

		γ-emission		β$^-$ emission		
Radionuclide	$\tau_{1/2}$ (d)	Energy (keV)	Intensity (%)	Mean energy (kev)	End point energy (keV)	Intensity (%)
^{48}Sc	1.819	983.526	100.1	158.6	483	10.02
		1037.522	97.6	227.3	659	89.98
		1212.880	2.38			
		1312.120	100.1			
^{47}Sc	3.349	159.381	68.3	142.6	440.9	68.4
				203.9	600.3	31.6
^{46}Sc	83.790	889.277	99.9840	111.8	356.9	99.9964
		1120.545	99.9870			

3.2 Calculation of the time dependence of the radionuclidic purity

The percentage of activity due to ^{47}Sc with respect to the total one is plotted as a function of time post irradiation in figure 2 for the different production conditions considered in table 1. It is clear that in all cases the RNP of ^{47}Sc decreases over time. For the two higher energy ranges (45-19 MeV and 40-19 MeV) the initial RNP is already lower than the 99% limit required by the European pharmacopoeia. For the wider energy range (45-19 MeV) the percentage of activity due to ^{47}Sc becomes lower than 90% just after 40 h and 65 h from the EOB, for 80 h and 24 h of irradiation respectively. By using the energy range 40-19 MeV this value is achieved after a longer time, about 130 h (for 80 h of irradiation) and 160 h (for 24 h of irradiation). When the proton energy range is restricted to 35-19 MeV the RNP is maintained higher than 99% up to 30 h and 60 h post EOB, respectively for 80 h and 24 h of irradiation, while RNP is kept higher than 99% up to 375 h and 400 h after EOB, respectively for 80 h and 24 h of irradiation, for beam energies 30-19 MeV.

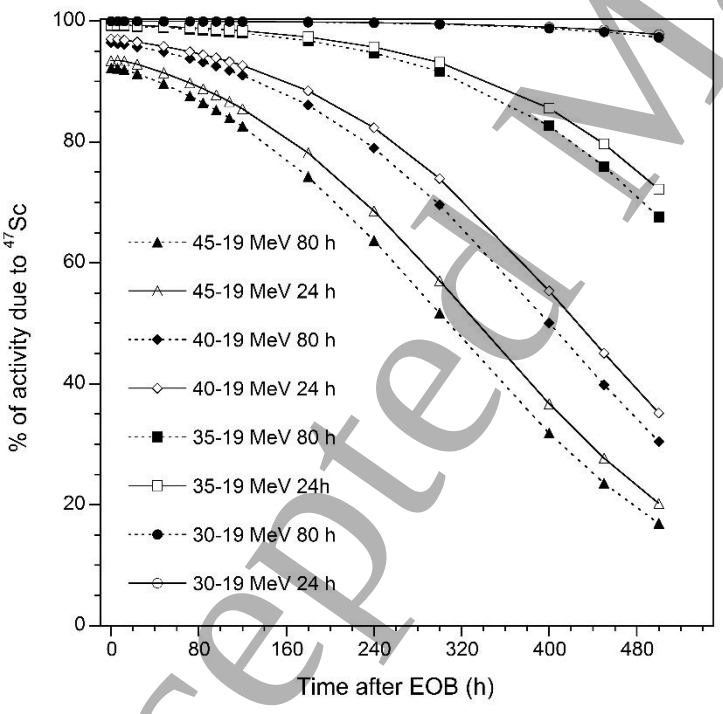

Figure 2. *Percentage of activity due to ^{47}Sc as a function of time post irradiation of thick ^{nat}V target, for irradiation with 1 μA proton beam, for different energy ranges and two irradiation times (80 h: full symbols, 24 h: empty symbols).*

3.3 Determination of the number of disintegrations in the source organs due to ^{xx}Sc-cm10 injection

Activity curves were obtained plotting the scaled radiopharmaceutical concentration vs. time for each source organ of the ICRP 89 male phantom (see figure 3). In general, organ activity curves show a fast radiopharmaceutical uptake with a slow wash-out, except for the heart contents, where the elimination was quite fast (see figure 3(b)).

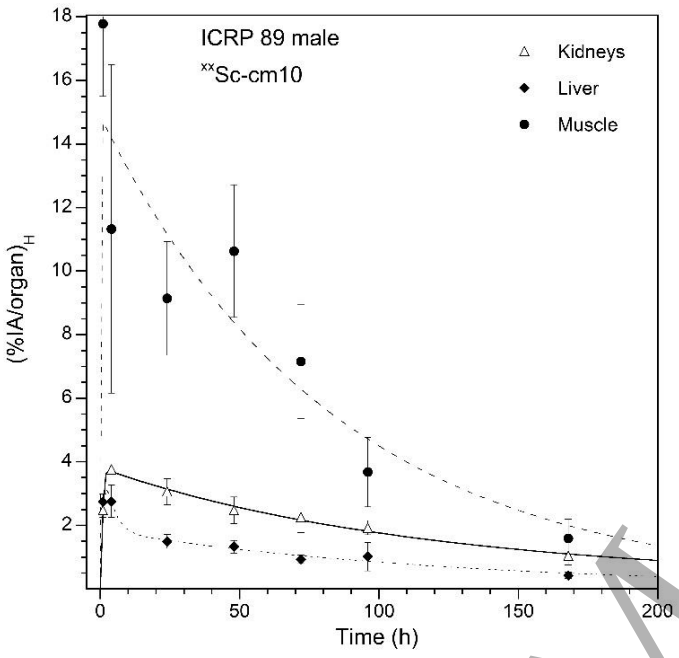

(a)

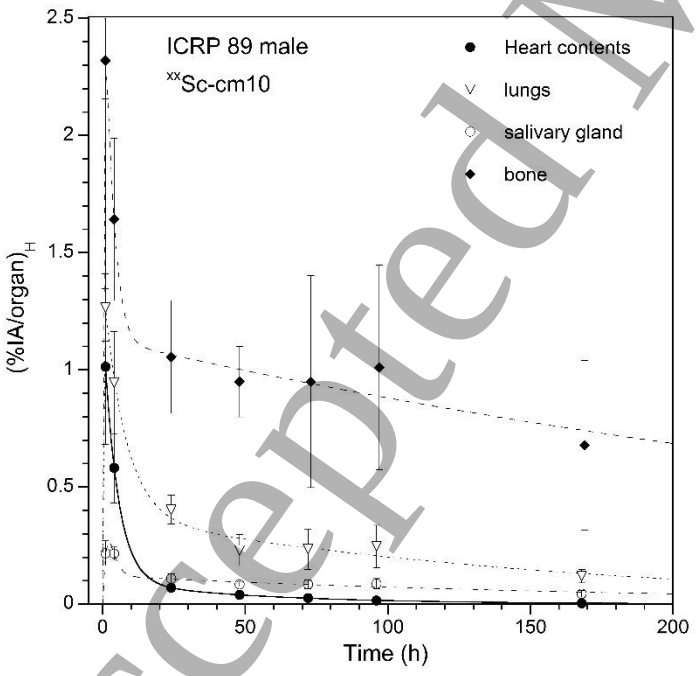

(b)

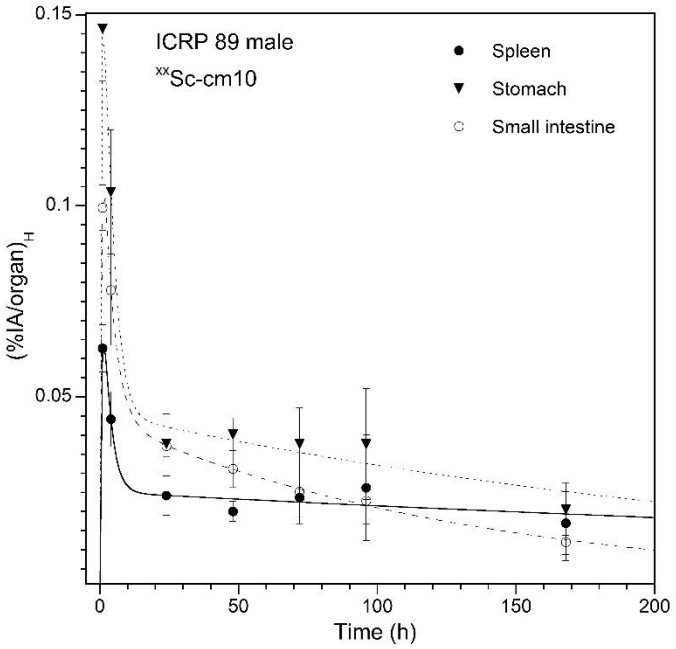

(c)

Figure 3. *$(\%IA/organ)_H$ values (symbols) of ^{xx}Sc-cm10 in the most important source organs for ICRP 89 male phantom plotted for each time p.i. and the organ activity curves (lines) obtained after the fitting. (a): Organs with high uptake: kidneys, liver, and muscle; (b): Organs with medium uptake: heart contents, lungs, salivary gland and bone; (c) Organs with low uptake: spleen, stomach and small intestine.*

The number of disintegrations in the source organs were calculated for ^{48}Sc, ^{47}Sc and ^{46}Sc, the three radionuclides expected to be produced through the proton irradiation of ^{nat}V target for $E_P \leq 45$ MeV (EXFOR 2020), assuming that the injected cm10 was labelled with only one of these isotopes (see Table 3).

ICRP 1979 suggest to assign bone activity of radionuclides with half-lives less than 10 days to bone surfaces and that of radionuclides with longer half-lives to bone volumes (ICRP 1979). Therefore, bone activity of ^{48}Sc and ^{47}Sc has been assigned to bone surfaces and that of ^{46}Sc to bone volumes (see ^{XX}Sc half-lives in table 2). The activity reported in the muscle after biodistribution studies was assigned to the "Remaining" organs when performing calculations with Olinda 2.1.1 because this tissue is not included in the source organs of the ICRP 89 phantom model. As the used biodistribution data do not include the whole-body activity of the mice or provide excretion data, the value of remaining activity evaluated

using only the muscle data may underestimate the whole-body activity. However, this choice is justified by the fact that both ex-vivo biodistribution studies and in vivo SPECT imaging studies published by Müller et al. (Müller *et al* 2014) demonstrate a very low retention of radioactivity beyond that considered in the listed source organs.

Table 3. *Number of nuclear transitions (MBq×h/MBq) in source organs per unit administered activity of ^{48}Sc-cm10, ^{47}Sc-cm10 and ^{46}Sc-cm10, for male ICRP 89 phantom.*

Tissues	^{48}Sc-cm10	^{47}Sc-cm10	^{46}Sc-cm10
Left colon	4.44×10^{-3}	6.30×10^{-3}	1.25×10^{-2}
Small Intestine	2.07×10^{-2}	2.94×10^{-2}	5.85×10^{-2}
Stomach	2.86×10^{-2}	4.28×10^{-2}	1.23×10^{-1}
Right colon	8.89×10^{-3}	1.26×10^{-2}	2.51×10^{-2}
Rectum	4.44×10^{-3}	6.30×10^{-3}	1.25×10^{-2}
Heart contents	7.89×10^{-2}	8.82×10^{-2}	1.06×10^{-1}
Kidneys	1.56×10^{0}	2.30×10^{0}	5.25×10^{0}
Liver	8.39×10^{-1}	1.18×10^{0}	2.32×10^{0}
Lungs	2.39×10^{-1}	3.25×10^{-1}	6.44×10^{-1}
Cortical bone	6.64×10^{-1}	1.07×10^{0}	4.02×10^{0}
Spleen	1.60×10^{-2}	2.63×10^{-2}	1.34×10^{-1}
Salivary glands	6.32×10^{-2}	9.38×10^{-2}	2.28×10^{-1}
Remaining	5.35×10^{0}	7.23×10^{0}	1.21×10^{1}

3.4 Organ absorbed doses and effective doses due to ^{48}Sc-cm10, ^{47}Sc-cm10 and ^{46}Sc-cm10

Table 4 presents the absorbed doses per unit administered activity in the main male organs calculated for ^{48}Sc-cm10, ^{47}Sc-cm10 and ^{46}Sc-cm10 with the OLINDA 2.1.1 software using the data of table 3. For ^{47}Sc-cm10 the organs receiving the highest absorbed doses are the kidneys, followed by the salivary glands and the liver. Both kidneys and salivary glands are normal tissues that show a limited expression of the folate receptor-α (Boss and Ametamey 2020), then the high values of absorbed dose to these organs are a consequence of their selective uptake and minimal wash-out of the Sc-cm10 radiopharmaceutical. Liver also frequently shows a high uptake of folate receptor–targeted radiopharmaceuticals, due to the expression of the proton-coupled folate transporter (PCFT) system in this organ. For ^{48}Sc-cm10 and ^{46}Sc-cm10 the organs with highest absorbed doses are also the kidneys but followed by the adrenals and then by the liver. Due to its longer half-life, the values of organ absorbed doses calculated for ^{46}Sc-cm10 are between 3.6 to 23.2 times higher than those

calculated for ^{47}Sc-cm10, making the ^{46}Sc-cm10 ED value about 7.7 times higher than the ^{47}Sc-cm10 ED. Despite ^{48}Sc shorter half-life, the absorbed dose values calculated for ^{48}Sc-cm10 are also higher than those calculated for ^{47}Sc-cm10, by a factor between 1.9 and 12, depending on the organ, due to the high-energy γ-emissions of ^{48}Sc (see Table 2). Therefore, ^{48}Sc-cm10 ED value is about 4.4 times higher than the ^{47}Sc-cm10 ED.

Table 4. *Organ absorbed doses per unit administered activity (mGy/MBq) and ED values per unit administered activity (mSv/MBq) calculated for ^{48}Sc-cm10, ^{47}Sc-cm10 and ^{46}Sc-cm10 with the OLINDA 2.1.1 software for male ICRP 89 phantoms using the data reported in table 3.*

Tissues	**^{48}Sc-cm10**	**^{47}Sc-cm10**	**^{46}Sc-cm10**
Adrenals	4.35×10^{-1}	3.62×10^{-2}	8.40×10^{-1}
Brain	6.10×10^{-2}	1.18×10^{-2}	1.02×10^{-1}
Esophagus	1.11×10^{-1}	1.47×10^{-2}	1.81×10^{-1}
Eyes	6.01×10^{-2}	1.18×10^{-2}	9.97×10^{-2}
Gallbladder Wall	1.93×10^{-1}	1.97×10^{-2}	3.24×10^{-1}
LLI Wall/Left Colon	1.43×10^{-1}	2.04×10^{-2}	2.47×10^{-1}
Small Intestine	1.22×10^{-1}	1.91×10^{-2}	1.99×10^{-1}
Stomach Wall	1.32×10^{-1}	2.35×10^{-2}	2.32×10^{-1}
ULI Wall/Right Colon	1.36×10^{-1}	2.00×10^{-2}	2.24×10^{-1}
Rectum	9.67×10^{-2}	1.75×10^{-2}	1.50×10^{-1}
Heart Wall	1.33×10^{-1}	2.31×10^{-2}	1.90×10^{-1}
Kidneys	1.39×10^{0}	7.29×10^{-1}	2.62×10^{0}
Liver	2.85×10^{-1}	7.36×10^{-2}	4.77×10^{-1}
Lungs	1.17×10^{-1}	3.00×10^{-2}	1.87×10^{-1}
Pancreas	1.45×10^{-1}	1.70×10^{-2}	2.48×10^{-1}
Prostate	9.65×10^{-2}	1.37×10^{-2}	1.48×10^{-1}
Salivary Glands	2.00×10^{-1}	1.07×10^{-1}	3.75×10^{-1}
Red Marrow	9.64×10^{-2}	1.13×10^{-2}	1.76×10^{-1}
Osteogenic Cells/Skeleton	1.27×10^{-1}	5.90×10^{-2}	3.24×10^{-1}
Spleen	1.89×10^{-1}	2.62×10^{-2}	4.28×10^{-1}
Testes	6.64×10^{-2}	1.18×10^{-2}	9.64×10^{-2}
Thymus	9.14×10^{-2}	1.32×10^{-2}	1.36×10^{-1}
Thyroid	8.02×10^{-2}	1.28×10^{-2}	1.24×10^{-1}
Urinary Bladder Wall	8.71×10^{-2}	1.31×10^{-2}	1.28×10^{-1}
Total Body	8.69×10^{-2}	1.96×10^{-2}	1.43×10^{-1}
ED (ICRP 103) (mSv/MBq)	1.12×10^{-1}	2.52×10^{-2}	1.93×10^{-1}

3.5 Calculation of the time dependence of the ED_t due to $^{48/47/46}$Sc-cm10 injection

Total ED (ED_t) for ICRP 89 male phantoms was calculated per unit of administered activity of the $^{48/47/46}$*Sc*-cm10 radiopharmaceutical considering the injection immediately after labelling with the mixtures of Sc-radioisotopes present at the different times after EOB.

$ED_t(t)$ calculated on the base of eq. (3) for all irradiation parameters reported on table 1 is showed in figure 4. ED_t increases very fast with time for the energy ranges 45-19 MeV and 40-19 MeV, for both 24 h and 80 h irradiation times, doubling its value between 200 h and 250 h after EOB. The increment is slower for the energy range 35-19 MeV and it becomes very weak in the energy window 30-19 MeV, with an increment at 500 h of only 14% and 18%, for 24 h and 80 h irradiation times respectively. The contribution of ^{47}Sc-radionuclide to ED_t is plotted in figure 5(a) at different time points after EOB. It is clear that for all production conditions, the ^{47}Sc-contribution to ED_t decreases with time, due to the increasing contribution of the long-lived ^{46}Sc-contaminant, as it can be observed in figure 5(b). ^{48}Sc was not produced when energies under 35 MeV are used for the irradiation. In addition, the small contribution to ED_t of ^{48}Sc produced with higher energies decreases with time, becoming completely negligible at about 40-50 h after EOB, due to the relatively short half-life of this radioisotope (figure 5(c)).

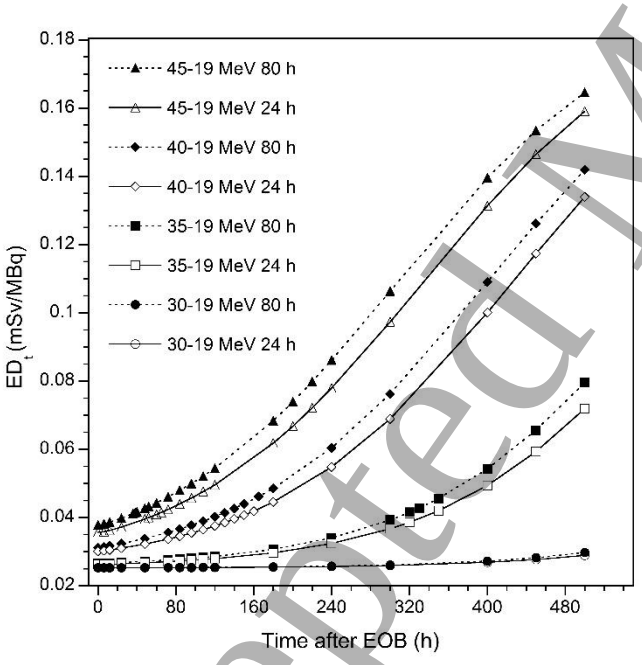

Figure 4. *Total ED (*ED_t**)** *(mSv/MBq) due to $^{48/47/46}$Sc-cm10 calculated for male adult ICRP 89 phantom, at different times after EOB, for irradiation with 1 μA proton beam for different energy ranges and two irradiation times (80 h: full symbols and 24 h: empty symbols).*

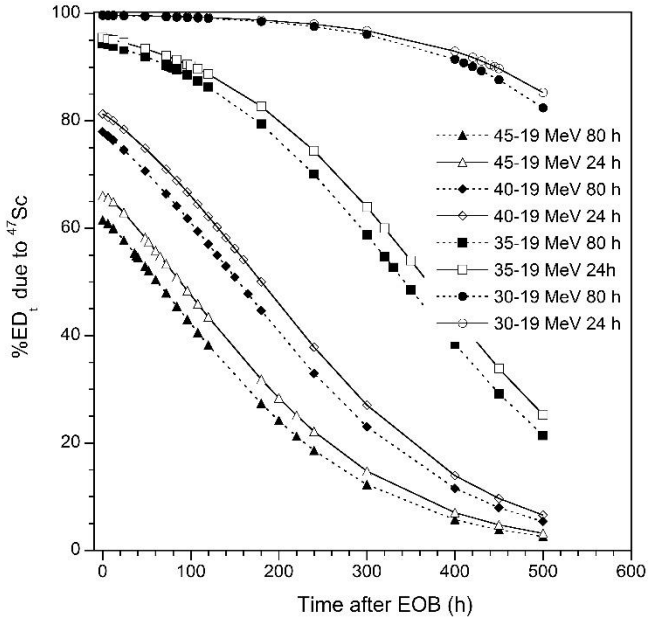

(a)

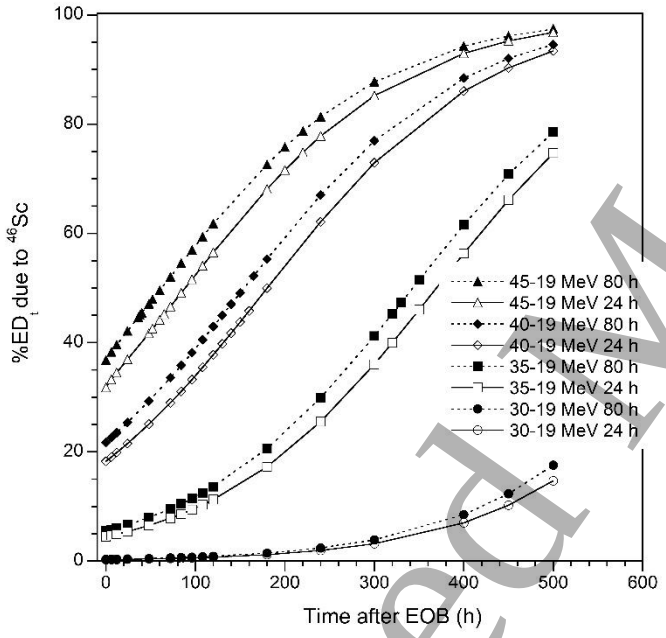

(b)

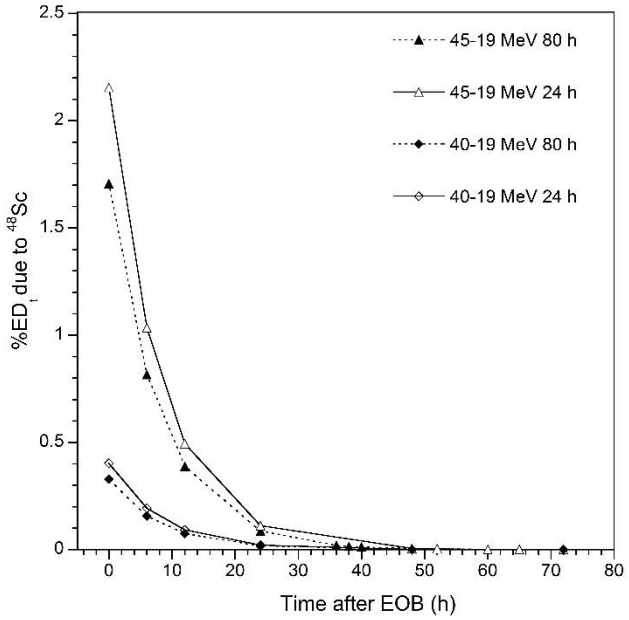

(c)

Figure 5. *Calculated contribution of Sc-radioisotopes ((a): ^{47}Sc; (b): ^{46}Sc; (c): ^{48}Sc) to the total ED (ED_t) using the male adult ICRP 89 phantom, at different times after EOB, for irradiation with 1 μA proton beam for different energy ranges and two irradiation times (80 h: full symbols and 24 h: empty symbols).*

4. Discussion

It has to be remembered that extreme care should always be taken when using biodistribution data from animals to predict absorbed doses to human organs. As already mentioned, the increment in the absorbed dose due to contaminant isotopes must be determined for each radiopharmaceutical, because it directly depends on the biodistribution and kinetics characteristics of the considered radiopharmaceutical. Despite these limitations, the results obtained in this study are useful to have an idea of the contribution of Sc impurities to the absorbed doses imparted to healthy individuals after injection of a ^{47}Sc-radiopharmaceutical and to select the irradiation conditions for ^{47}Sc production through ^{nat}V(p,x)^{47}Sc cyclotron irradiation that will be further investigated by experimental measurements. The calculated yields of ^{47}Sc and contaminants (^{46}Sc and ^{48}Sc) show that the RNP of ^{47}Sc at the EOB is higher than 99% just for two of the irradiation conditions considered in Table 1, suggesting that proton energies below 35 MeV must be used to

produce this radioisotope through irradiation of a ^{nat}V target. In this energy range only ^{46}Sc is produced as impurity.

In addition, assuming as acceptable that the ^{47}Sc contribution to the ED_t due to a Sc-radiopharmaceutical can not be lower than 90%, the results in figure 5(a) in the 35-19 MeV energy range suggest that it can be considered acceptable to label and inject Sc-cm10 radiopharmaceutical up to 78 h (for 80 h irradiation) or up to 100 h (for 24 h irradiation) after EOB. When the energy range is reduced to 30-19 MeV, the interval of time can be extended up to 420 h or 445 h after EOB, respectively for 80 h and 24 h irradiation. However, when considering the criterion that guarantees a RNP>99%, the results plotted in Figure 2 show that in the 35-19 MeV energy range the time t_{max} reduces to about 30 h after EOB, for 80 h irradiation, and to 60 h after EOB, for 24 h irradiation. When the energy range is reduced to 30-19 MeV the interval of time can be extended up to 375 h or 400 h after EOB, for 80 h and 24 h irradiation respectively. Therefore, for this ^{47}Sc production route and the considered radiopharmaceutical, the 99% limit regarding the RNP is more restrictive than the 90% limit regarding the ^{47}Sc contribution to the ED_t, especially in the case of the 35-19 MeV energy window. The values of t_{max} evaluated with the more restrictive criterion (RNP>99%) are summarized in table 5, together with the activity of ^{47}Sc produced at EOB with a proton current of 100 μA. For each energy window, the time t_{max} is higher for 24 h irradiation compared to 80 h, but for shorter irradiation time the amount of ^{47}Sc produced is lower. Comparing both energy windows, it is confirmed that the amount of ^{47}Sc produced is higher for the 35-19 MeV energy range, but at the expense of a shorter t_{max}. The amount of ^{47}Sc activity produced in this energy range, with 100 μA current and 80 h irradiation of a ^{nat}V target, is much higher (27.9 GBq) than that obtained after a comparable time of irradiation (3.94 d) of a ^{46}Ca target (1 mg) at a high-flux reactor (0.6 GBq at the end of irradiation) (Müller *et al* 2014). Besides, a main drawback of the ^{47}Sc production through the ^{46}Ca(n,γ)^{47}Ca ($\tau_{1/2}$= 4.536 d) → ^{47}Sc reaction is the low natural abundance of the target isotope (0.004%), requiring enriched targets with high cost and which would require recycling. In contrast, the ^{nat}V(p,x)^{47}Sc production route employs a low-cost and easily available material and it does not need the use of a reactor.

Table 5. *Calculated yields at EOB of ^{47}Sc obtained with ^{nat}V thick targets irradiated with proton beams in the energy range 35-19 MeV and 30-19 MeV (I_P = 100 μA, t_{IRR} = 80 h and 24 h), the time t_{max}(h) corresponding to the limit of a RNP of 99% and the ED_t due to the $^{47/46}Sc$-cm10 radiopharmaceutical per unit of administered activity at EOB.*

Energy range (MeV)	t_{IRR} = 80 h, I_P = 100 μA			t_{IRR} = 24 h, I_P = 100 μA		
	^{47}Sc (GBq)	t_{max} (h)	ED_t (mSv/MBq) at EOB	^{47}Sc (GBq)	t_{max} (h)	ED_t (mSv/MBq) at EOB
35-19	27.9	30	2.65×10^{-2}	10.5	60	2.62×10^{-2}
30-19	11.1	375	2.53×10^{-2}	4.15	400	2.53×10^{-2}

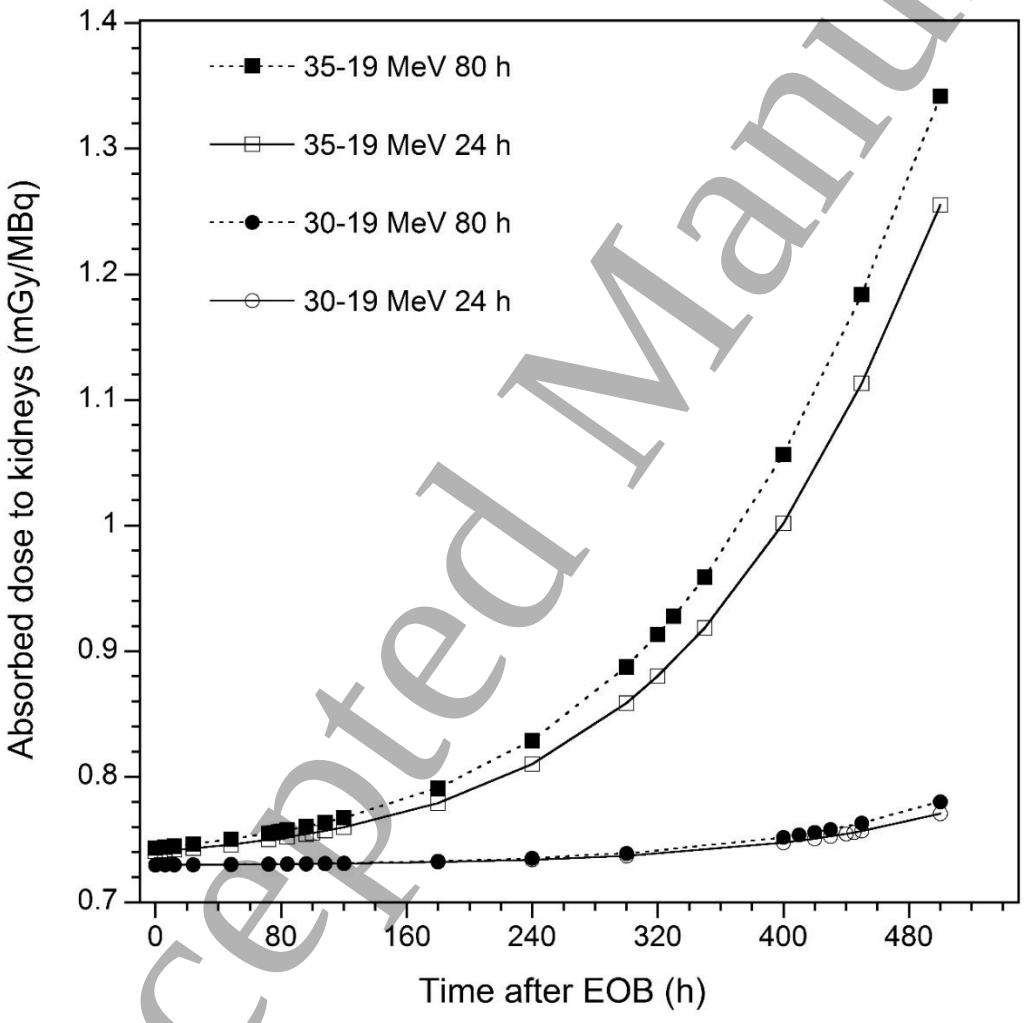

(a)

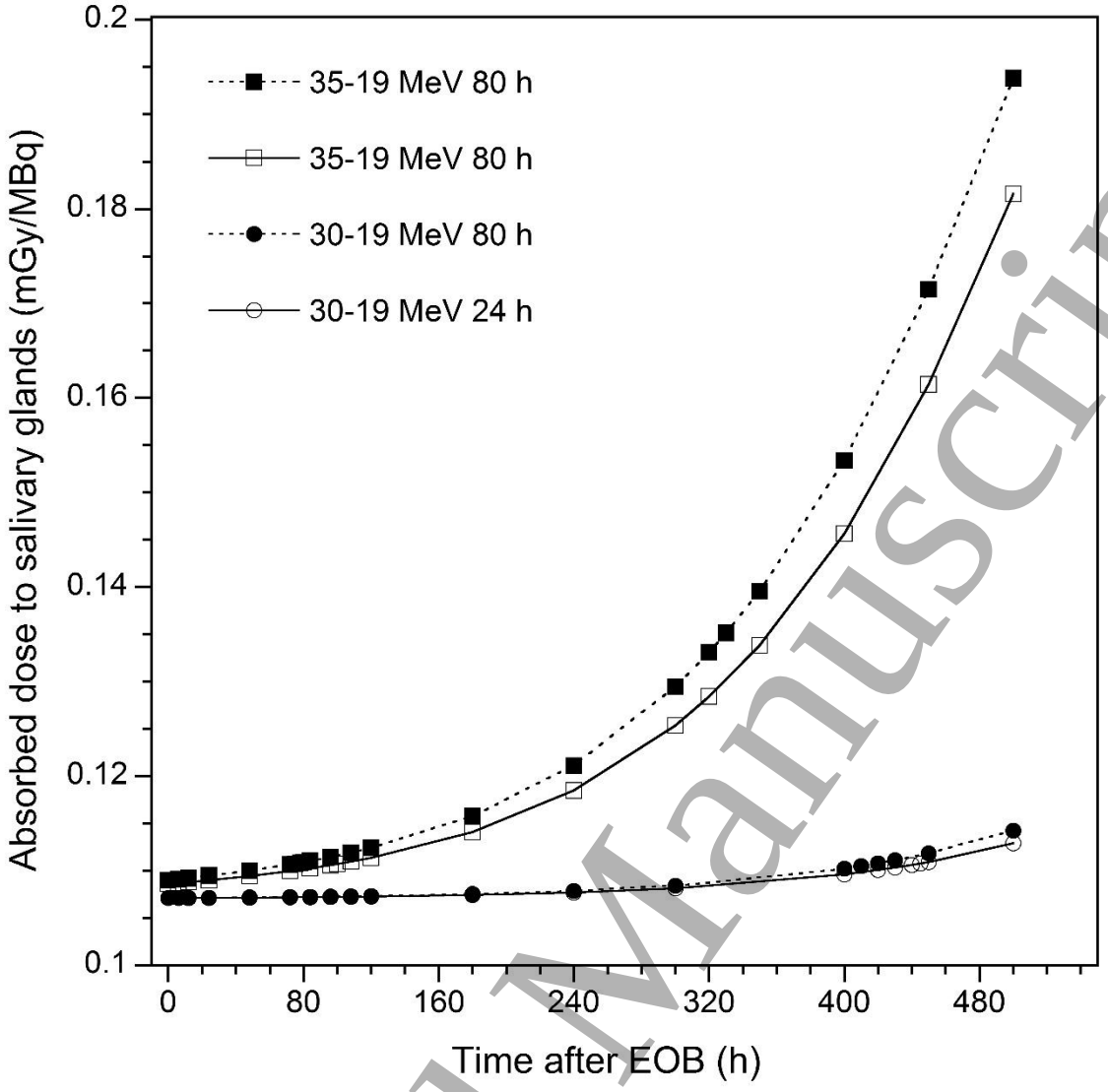

(b)

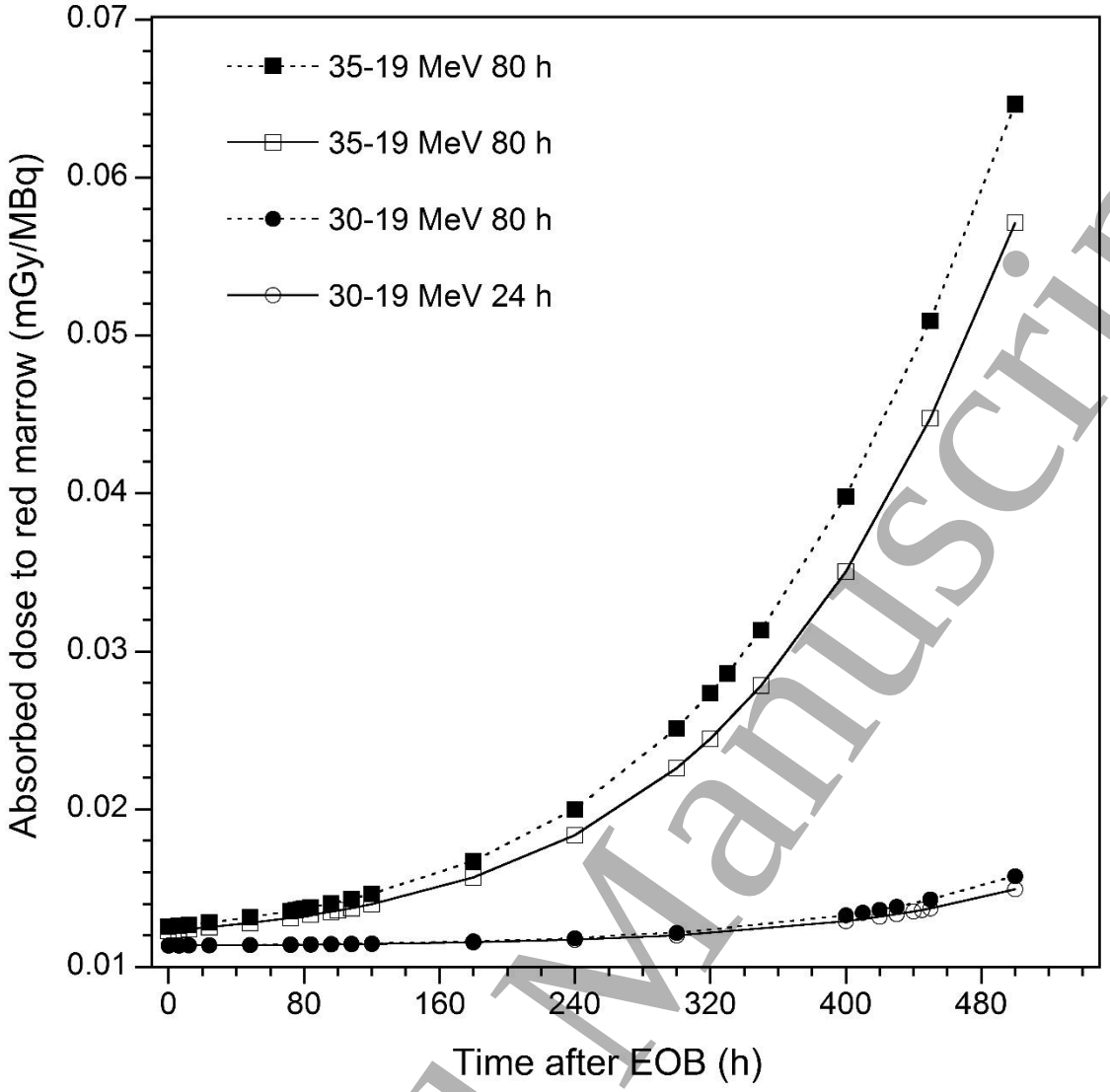

(c)

Figure 6. *Absorbed dose per unit administered activity (mGy/MBq) to kidneys (a), salivary glands (b) and red marrow (c) due to $^{47/46}$Sc-cm10 radiopharmaceutical, calculated for male adult ICRP 89 phantom, at different times after EOB, for 35-19 MeV and 30-19 MeV energy ranges and two irradiation times (80 h: full symbols and 24 h: empty symbols).*

Table 5 also shows that the total ED due to the $^{47/46}$Sc-cm10 radiopharmaceutical per unit of administered activity is between 2.53×10^{-2} and 2.65×10^{-2} mSv/MBq at EOB. The total ED increases to about 2.68×10^{-2} mSv/MBq at t_{max} (see figure 4), anyway this value remains comparable to that reported for other theranostic radiopharmaceuticals, such as ^{177}Lu-iPSMA (ED=4×10^{-2} mSv/MBq (Santos-Cuevas *et al* 2018)). In the same time interval, the

absorbed dose per unit administered activity to the kidneys increases from about 0.74 mGy/MBq to about 0.75 mGy/MBq, for the salivary glands from about 0.107 mGy/MBq to about 0.110 mGy/MBq and for the red marrow from about 0.012 mGy/MBq to about 0.013 mGy/MBq (see figure 6). The absorbed doses per unit administered activity for liver and total body are respectively about 0.074 mGy/MBq and 0.020 mGy/MBq at EOB and increase to about 0.078 mGy/MBq and 0.021 mGy/MBq respectively at t_{max}. As it can be observed in figures 4 and 6, the ED and organ absorbed doses increase occur for both 35-19 MeV and 30-19 MeV energy windows, but it is much faster for the 35-19 MeV irradiation. However, a much lower value of t_{max} in the 35-19 MeV case (see Table 5) guarantees for both irradiation conditions similar values of ED and absorbed doses at t_{max}. Considering that the established tolerance limits derived from external beam radiotherapy and ^{177}Lu radionuclide therapy are between 23-40 Gy for kidneys, 25-35 Gy for salivary glands, 30 Gy for liver and 2 Gy for both bone marrow and whole body (Kratochwil *et al* 2019, Khawar *et al* 2018), the dose limiting organs for ^{47}Sc-cm10 appear to be the kidneys. The absorbed dose values per unit administered activity for kidneys are however comparable with those reported in the literature for others theranostic agents as ^{177}Lu-PSMA-617, ^{177}Lu-PSMA-I&T (mean value= 0.5±0.2 mGy/MBq (Kratochwil *et al* 2019)) and ^{177}Lu-iPSMA (0.880 mGy/MBq (Santos-Cuevas *et al* 2018)), low molecular weight PSMA-ligands radiolabelled with the β^- particle emitter ^{177}Lu used for prostate cancer treatment. Generally, the administered activity per treatment with these radiopharmaceuticals is in the range 3.7–9.3 GBq (100–250 mCi) (Kratochwil *et al* 2019), but about 25% higher activity of ^{47}Sc-labelled radiopharmaceutical should be injected to have a comparable absorbed dose to the tumor (Siwowska *et al* 2019). Even considering this higher activity and supposing a treatment with 11.625 GBq (i.e. 9.3 GBq×1.25) of $^{47/46}$Sc-cm10 radiopharmaceutical performed at $t_{max,}$ the absorbed dose in the kidneys, salivary glands, liver, bone marrow and whole body are much lower than the absorbed dose limits previously mentioned, as evidenced in table 6. Taking into account the activity required per treatment, the amount of ^{47}Sc activity produced for 80 h irradiation of ^{nat}V target with 100 μA of 35-19 MeV protons should be enough for 2-6 treatments.

Therefore, the cyclotron produced ^{47}Sc could be a cheaper alternative to the reactor produced ^{177}Lu to label theranostic agents.

It must be pointed out that these results were obtained considering only the male phantom and not the female one. Effective doses are expected to be on average 25% higher for female (Stabin 1997), due to female's overall body and organ sizes, which are smaller and closer than those of males and to the collocation of female gonads inside the body, near to several source organs. So, according to the ICRP definition of ED as a sex-averaged quantity (ICRP 2007), 10-15% higher values of ED should be expected with respect to those reported in this work. However, the general dependence of ICRP-ED on beam energy and time after EOB as well as the final evaluation of the time window (t_{max}) will be unchanged.

Table 6. *Calculated absorbed dose in the main organs (Gy) after a therapeutic treatment with $^{47/46}$Sc-cm10 radiopharmaceutical (11.625 GBq) performed at t_{max} and comparison with the absorbed dose limits values (Gy).*

Organs	Absorbed dose per unit administered activity at t_{max} (Gy/GBq)	Absorbed dose (Gy) per treatment (11.625 GBq)	Dose limits (Gy)
Kidneys	0.750	8.719	23-40
Salivary glands	0.110	1.279	25-35
Liver	0.078	0.907	30
Bone marrow	0.013	0.151	2
Whole body	0.021	0.244	2

5. Conclusions

Imposing the limits of 99% for the radionuclidic purity and 10% for the contribution of radioactive Sc-contaminants to the total effective dose, proton energies below 35 MeV must be operated to produce ^{47}Sc by irradiation of ^{nat}V target. In particular, for this ^{47}Sc production route and the considered radiopharmaceutical, the 99% limit regarding the RNP has been found to be more restrictive than the 10% limit regarding the Sc-contaminants contribution to the ED_t for the evaluation of the time window (t_{max}) after the EOB in which a ^{47}Sc-labeled radiopharmaceutical could be injected. Using the over mentioned conditions, the assessed values of ED_t and kidneys absorbed dose per unit administered activity of ^{47}Sc-cm10 are

comparable to those reported for other theranostic agents. As regard to the time of irradiation, 80 h is preferable to 24 h, because the amount of ^{47}Sc produced is much higher even if the time t_{max} is shorter (see table 5). Besides, if the amount of ^{47}Sc produced is a priority with respect of having a long t_{max}, the wider energy window 35-19 MeV should be preferred to the energy range 30-19 MeV.

To confirm the Thick Target Yield (TTY) estimation performed in this work for ^{xx}Sc radionuclides based on experimental cross section data of the ^{nat}V(p,x)^{xx}Sc nuclear reactions, production yields measurements of ^{47}Sc and its contaminants are planned to be performed in a dedicated experiment at the ARRONAX facility (Haddad *et al* 2008), exploiting the low current proton beam-line devoted to nuclear cross section measurements. Besides, a more accurate dosimetric analysis, including calculations for female phantom, will be performed when these experimental yields data or more accurate biodistribution data, including whole-body activity, will be available.

Acknowledgments

This work has been partially supported by Istituto Nazionale di Fisica Nucleare CSN5 with the Grant PASTA (Bando Giovani Ricercatori No. 18203).

References

EANM 2019 Radiopharmacy: An Update. Published by European Association of Nuclear Medicine, available at: https://www.eanm.org/publications/technologists-guide/radiopharmacy-an-update/

EDQM 2018 Guide for the elaboration of monographs on radiopharmaceutical preparations. European Pharmacopoeia. European Directorate for the Quality of Medicines & HealthCare (EDQM) Edition 2018, available at: https://www.edqm.eu/sites/default/files/guide_-_guide_for_the_elaboration_of_monographs_on_radio-pharmaceutical_preparations_-_october_2018.pdf

European Pharmacopeia 2018. Sodium pertechnetate (99mTc) injection (accelerator-produced) natrii pertechnetatis (99mTc) acceleratore formati solutio iniectabilis. Ph. Eur. 10th edition 01/2018:2891

EXFOR 2020 Experimental Nuclear Reaction Data (EXFOR) Database, available at: https://www-nds.iaea.org/exfor/exfor.htm

Boss S D and Ametamey S M 2020 Development of folate receptor–targeted PET radiopharmaceuticals for tumor imaging—a bench-to-bedside journey *Cancers (Basel).* **12** 1–20 Online: www.mdpi.com/journal/cancers

Haddad F, Ferrer L, Guertin A, Carlier T, Michel N, Barbet J and Chatal J F 2008 ARRONAX, a high-energy and high-intensity cyclotron for nuclear medicine *Eur. J. Nucl. Med. Mol. Imaging* **35** 1377–87

IAEA 2014 CRP IAEA , IAEA Coordinated Research Project (CRP) on "Therapeutic Radiopharmaceuticals Labelled with New Emerging Radionuclides (67Cu, 186Re, 47Sc)" (IAEA CRP No. F22053).

IAEA T R S N 465 2008 *Cyclotron Produced Radionuclides: Principles and Practice*

IAEA T R S N 468 2009 *Cyclotron Produced Radionuclides: Physical Characteristics and Production Methods*

ICRP 2002 *Basic Anatomical and Physiological Data for Use in Radiological Protection Reference Values. ICRP Publication 89. Ann. ICRP 32 (3-4).* Online: http://www.icrp.org/publication.asp?id=ICRP Publication 89

ICRP 1979 *Limits for Intakes of Radionuclides by Workers. ICRP Publication 30*

ICRP 2007 *The 2007 Recommendations of the International Commission on Radiological Protection. ICRP Publication 103. Ann. ICRP 37 (2-4).* Online: http://www.icrp.org/publication.asp?id=ICRP Publication 103

Khawar A, Eppard E, Sinnes J P, Roesch F, Ahmadzadehfar H, Kürpig S, Meisenheimer M,

Gaertner F C, Essler M and Bundschuh R A 2018 Prediction of Normal Organ Absorbed Doses for [177Lu]Lu-PSMA-617 Using [44Sc]Sc-PSMA-617 Pharmacokinetics in Patients with Metastatic Castration Resistant Prostate Carcinoma *Clin. Nucl. Med.* **43** 486–91

Kratochwil C, Fendler W P, Eiber M, Baum R, Bozkurt M F, Czernin J, Delgado Bolton R C, Ezziddin S, Forrer F, Hicks R J, Hope T A, Kabasakal L, Konijnenberg M, Kopka K, Lassmann M, Mottaghy F M, Oyen W, Rahbar K, Schöder H, Virgolini I, Wester H J, Bodei L, Fanti S, Haberkorn U and Herrmann K 2019 EANM procedure guidelines for radionuclide therapy with 177Lu-labelled PSMA-ligands (177Lu-PSMA-RLT) *Eur. J. Nucl. Med. Mol. Imaging* **46** 2536–44 Online: https://doi.org/10.1007/s00259-019-04485-3

Meléndez-Alafort L, Ferro-Flores G, De Nardo L, Bello M, Paiusco M, Negri A, Zorz A, Uzunov N, Esposito J and Rosato A 2019 Internal radiation dose assessment of radiopharmaceuticals prepared with cyclotron-produced 99m Tc *Med. Phys.* **46** 1437–46

Meléndez-Alafort L, Rosato A, Ferro-Flores G, Penev I and Uzunov N 2017 Development of a five-compartmental model and software for pharmacokinetic studies *Comptes Rendus L'Academie Bulg. des Sci.* **70** 1649–54

Mikolajczak R, van der Meulen N P and Lapi S E 2019 Radiometals for imaging and theranostics, current production, and future perspectives *J. Label. Compd. Radiopharm.* **62** 615–34

Müller C, Bunka M, Haller S, Koster U, Groehn V, Bernhardt P, van der Meulen N, Turler A and Schibli R 2014 Promising Prospects for 44Sc-/47Sc-Based Theragnostics: Application of 47Sc for Radionuclide Tumor Therapy in Mice *J. Nucl. Med.* **55** 1658–64 Online: http://jnm.snmjournals.org/content/55/10/1658.full.pdf

Notni J and Wester H J 2018 Re-thinking the role of radiometal isotopes: Towards a future concept for theranostic radiopharmaceuticals *J. Label. Compd. Radiopharm.* **61** 141–53

Pupillo G, Mou L, Boschi A, Calzaferri S, Canton L, Cisternino S, De Dominicis L, Duatti A, Fontana A, Haddad F, Martini P, Pasquali M, Skliarova H and Esposito J 2019 Production of 47Sc with natural vanadium targets: results of the PASTA project *J. Radioanal. Nucl. Chem.* **322** 1711–8 Online: https://doi.org/10.1007/s10967-019-06844-8

Qaim S M, Scholten B and Neumaier B 2018 New developments in the production of theranostic pairs of radionuclides *J. Radioanal. Nucl. Chem.* **318** 1493–509 Online: https://doi.org/10.1007/s10967-018-6238-x

Santos-Cuevas C, Ferro-Flores G, García-Pérez F O, Jiménez-Mancilla N, Ramírez-Nava G, Ocampo-García B, Luna-Gutiérrez M, Azorín-Vega E, Davanzo J and Soldevilla-Gallardo I 2018 177 Lu-DOTA-HYNIC-Lys(Nal)-Urea-Glu: Biokinetics, Dosimetry, and Evaluation in Patients with Advanced Prostate Cancer *Contrast Media Mol. Imaging* **2018**

Siwowska K, Guzik P, Domnanich K A, Rodríguez J M M, Bernhardt P, Ponsard B, Hasler R, Borgna F, Schibli R, Köster U, Van Der Meulen N P and Müller C 2019 Therapeutic potential of 47Sc in comparison to 177Lu and 90Y: Preclinical investigations *Pharmaceutics* **11** 1–13

Sparks R and Aydogan B 1999 Comparison of the effectiveness of some common animal data scaling techniques in estimating human radiation dose *Sixth international radiopharmaceutical dosimetry symposium* pp 705–16

Stabin M and Farmer A 2012 OLINDA/EXM 2.0: The new generation dosimetry modeling code *J. Nucl. Med.* **53** 585–585 Online: http://jnm.snmjournals.org/content/53/supplement_1/585.abstract?sid=61dd62a5-0bc2-4a78-ae1d-8406ad9619b1

Stabin M G 1997 *Health Concerns Related to Radiation Exposure of the Female Nuclear Medicine Patient* vol 105 Online: https://www.ncbi.nlm.nih.gov/pmc/articles/PMC1469927/pdf/envhper00331-0031.pdf

Stabin M G, Sparks R B and Crowe E 2005 OLINDA/EXM: The Second-Generation Personal Computer Software for Internal Dose Assessment in Nuclear Medicine *J Nucl Med* **46** 1023–7 Online: http://jnm.snmjournals.org/content/46/6/1023.full.pdf

Stabin M G, Xu X G, Emmons M A, Segars W P, Shi C and Fernald M J 2012 RADAR Reference Adult, Pediatric, and Pregnant Female Phantom Series for Internal and External Dosimetry *J. Nucl. Med.* **53** 1807–13 Online: http://jnm.snmjournals.org/cgi/doi/10.2967/jnumed.112.106138

Stabin M and Siegel J A 2017 Radar Dose Estimate Report: a Compendium of Radiopharmaceutical Dose Estimates Based on Olinda/Exm Version 2.0 *J. Nucl. Med.* **59** 154–60 Online: http://jnm.snmjournals.org/lookup/doi/10.2967/jnumed.117.196261

Yordanova A, Eppard E, Kürpig S, Bundschuh R A, Schönberger S, Gonzalez-Carmona M, Feldmann G, Ahmadzadehfar H and Essler M 2017 Theranostics in nuclear medicine practice *Onco. Targets. Ther.* **10** 4821–8